Reconstruction of the Jaynes-Cummings field state of ionic motion in a harmonic trap

Dingshun Lv[1],Shuoming An[1], Mark Um[1], Junhua Zhang[1], Jing -Ning Zhang[1], M. S. Kim[2*] & Kihwan Kim[1†]
1. Center for Quantum Information, Institute for Interdisciplinary Information Sciences, Tsinghua University, Beijing 100084, P. R. China and
2. QOLS, Blackett Laboratory, Imperial College London, SW7 2AZ, United Kingdom

We experimentally measure the Q-function and reconstruct the Wigner function of the phononic state of the vibrational motion for an $^{171}Yb^{+}$ ion *resonantly* interacting with its internal energy states. The scheme for the Q-function is based on highly efficient vacuum phonon detection using the transitionless adiabatic passage on the external motion-internal states interaction. The Jaynes-Cummings dynamics of entanglement between the external and internal states has been known to bring the state of the field to a superposition of two composite states, which are nearly coherent states. The measured Q-function clearly shows two peaks in phase space at a certain interaction time and the quantum superposition of this state is confirmed by the reconstruction of the Wigner function with negativities manifesting the quantum interferences between the two composite states. The scheme can be applied to other physical setups including circuit-QED and opto-mechanical systems.

PACS numbers: 03.65.Ta, 37.10.Ty, 42.50.Dv, 42.50.Md

One of the most fundamental interaction models in quantum mechanics is the so-called Jaynes-Cummings model (JCM)[1], where a single two-level atom resonantly interacts with a single-mode field. The JCM has enabled the theoretical and experimental investigations of the basic properties of quantum electrodynamics such as Rabi oscillations of the energy transfer between the two subsystems and collapses and revivals of the oscillations [2]. More recently, the model has been widely studied for its rich properties of quantum control, coherent superposition and entanglement which are closely related to the current development of quantum technology. In order to see the nonclassical effects due to quantum interaction, the JCM is often studied with the state initially prepared in a coherent field, which is normally considered as the most classical state among all the pure quantum states and the atom in its energy eigenstate. It has been shown that the field and the atom are entangled [3] as soon as the interaction starts, but at a certain time they are nearly disentangled to bring the field into a superposition of two coherent states of π phase difference [4, 5]. Earlier, Eiselt and Risken [6, 7] showed that the Gaussian probability distribution of the initial coherent state in phase space breathe at the very initial points of interaction, reflecting the Rabi oscillations. Then the Gaussian peak bifurcates to travel around a circle in opposite direction in phase space. The bifurcation is a consequence of quantum nature of interaction and was experimentally probed through the measurement of field phase distribution [8–10]. However, the full reconstruction of the dynamics of the JCM field has not been experimentally demonstrated.

A phase-space reconstruction of the density operator of a field can be performed by the measurement of quasi-probabilities, such as the Husimi Q and the Wigner functions [11]. There have been many developments of reconstructing the quantum state of a field in various systems and situations. In particular, when the interaction is off-resonant with the dispersive coupling, a coherent superposition was realized in an atom-field interaction model [12, 13] and a scheme to reconstruct the quantum state has been developed [14]. Recently, in superconducting circuit-QED systems, such coherent superpositions and state reconstructions have also been demonstrated [15–17]. For phononic states of a trapped ion in a harmonic potential, a direct reconstruction of density matrix and Wigner function was demonstrated [18]. Under the resonant condition of JCM, however, none of these schemes were applied to monitor the dynamics.

The definition of the Q-function is $Q(\alpha) = \frac{1}{\pi}\langle 0|\hat{D}^{\dagger}(\alpha)\hat{\rho}\hat{D}(\alpha)|0\rangle$, where $\hat{D}(\alpha)$ is the displacement operator [19]; the value of the Q-function is merely the weight of the vacuum component of a given state once it is displaced in phase space. The measurement of nothing is, however, not straightforward. If the cavity has no photons, an atom initially prepared in its ground state will remain there forever. However, by merely measuring the atom in its ground state we cannot say that the cavity is empty because the Rabi oscillations periodically bring the atom back to the ground state even with many photons in the cavity. The oscillation frequency depends on how many photons are present in the cavity. The authors in Ref. [8–10] suggested that at a certain interaction time if there are photons, the atom initially in its ground state will be excited with approximately 50% probabilities. Thus at this time, if the atoms are found in the ground state, it is likely that the cavity is in the vacuum. However, this method works approximately for a very small number of photons ($n \leq 4$) and relies on their experimental perfections [8–10].

Here, we realize the highly efficient vacuum detection using the transitionless adiabatic passage scheme [20–22] on the phononic state in the dynamics of the JCM with

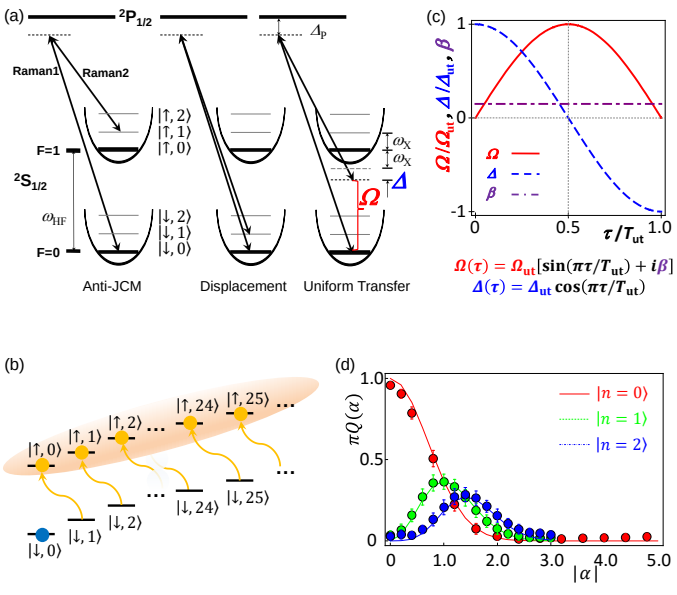

FIG. 1: **Raman laser schemes and the vacuum measurement.** (a) The Hilbert space of the system is comprised of the direct product of qubit states $\{|\downarrow\rangle, |\uparrow\rangle\}$ and phonon number states $\{|n=0\rangle, |1\rangle, |2\rangle, ...\}$. Raman laser beams, which have σ_- polarization and are detunned by $\Delta_p \approx 12.9$ THz from the $P_{1/2}$ manifold, perform anti-JCM, displacement operation and the vacuum measurement by adjusting their beating frequencies. (b) The vacuum component is measured by transferring the population of $|\downarrow, n\rangle$ to that of $|\uparrow, n-1\rangle$ for any value of n at the same duration of pulse. The atom remaining in no fluorescence state $|\downarrow\rangle$ indicates the phononic state being in $|0\rangle$. (c) The uniform transfer for any phononic state $|n\rangle$ to $|n-1\rangle$ is accomplished by the scheme of shortcuts to the adiabaticity, where $\Omega_{ut} = (2\pi)22.7$ kHz, $\beta = 0.075$, $\Delta_{ut} = 1.9\Omega_{ut}$ and the total duration $T_{ut} = 198.2\mu$s. (d) The Q-function of phononic Fock state $n = 0, 1, 2$ depending on the absolute amount of displacement $|\alpha|$. The points with error bars are the experimental results while the dashed lines are by the theory. The error bars are obtained by the standard deviation of the quantum projection noise with 100 repetitions.

a trapped ion. The demonstrated adiabatic passage [22] has been significantly improved in order to measure the vacuum of a reasonably large phonon state when there are up to ~ 25 phonons, which is necessary for the Q-function measurements. In order to clearly show the quantum interference in phase space, we also develop a method to reconstruct the density matrix and the Wigner function. The phonon number distribution is obtained by the Fourier transformation of the Rabi oscillations as in [18]. With the phonon number distributions after displacements we reconstruct the Wigner function. While the Q-function is directly measured efficiently (near perfect accuracy for 100 data takings), the numerically reconstruction of the Wigner function is slow and less efficient.

We employ the vibrational mode of a single trapped ion $^{171}Yb^+$ in a harmonic potential with the frequency of $\omega_X = (2\pi)$ 2.8 MHz. We encode the qubit state into two hyperfine states $|F=1, m_F=0\rangle \equiv |\uparrow\rangle$ and $|F=0, m_F=0\rangle \equiv |\downarrow\rangle$ of the $S_{1/2}$ manifold with the transition frequency $\omega_{HF} = (2\pi)$ 12.6428 GHz. We realize the JCM or anti-JCM by applying a pair of counter-propagating Raman beams that have the frequency differences of $(\omega_{R1} - \omega_{R2}) = \omega_{HF} \mp \omega_X$, respectively, as shown in Fig. 1(a). In the interaction picture, the Raman laser interactions can be described by the following JCM and anti-JCM Hamiltonians

$$\begin{aligned} \hat{H}_{JC}(\phi) &= \frac{\hbar\eta\Omega}{2}\left(\hat{a}\hat{\sigma}_+ e^{i\phi} + \hat{a}^\dagger\hat{\sigma}_- e^{-i\phi}\right), \\ \hat{H}_{aJC}(\phi) &= \frac{\hbar\eta\Omega}{2}\left(\hat{a}^\dagger\hat{\sigma}_+ e^{i\phi} + \hat{a}\hat{\sigma}_- e^{-i\phi}\right). \end{aligned} \quad (1)$$

Here, $\hat{a}^\dagger$ and $\hat{a}$ are the phonon creation and annihilation operators, $\hat{\sigma}_+ (\hat{\sigma}_-) = |\uparrow\rangle\langle\downarrow| (|\downarrow\rangle\langle\uparrow|)$ are spin-raising (lowering) operator and Ω the vacuum Rabi frequency of (anti-)JCM, $\eta = \Delta k\sqrt{\hbar/M\omega_X}$ the Lamb-Dicke parameter with Δk the net wave-vector of the Raman laser beams, M the mass of the $^{171}Yb^+$ ion and ϕ is the phase difference of the Raman laser beams.

The essence of the vacuum-component measurement is in the realization of the uniform population transfer of $|\downarrow, n\rangle \rightarrow |\uparrow, n-1\rangle$ for any n as shown in Fig. 1(b). After the uniform transfer, all the phonon states except the vacuum component $|n=0\rangle$ are in the bright electronic state $|\uparrow\rangle$, which emits photons during the standard fluorescence detection sequence. Therefore, the atom being in the dark electronic state $|\downarrow\rangle$ after the uniform transfer indicates the phonon state in the vacuum. By measuring the vacuum probability of the state after displacing it by α, we can directly measure the Q-function $Q(\alpha)$.

In general, the frequency of the Rabi oscillations between $|\downarrow, n\rangle$ and $|\uparrow, n-1\rangle$ has $\sqrt{n}$ dependency due to the nature of JCM coupling. To accomplish the uniform transfer, we basically apply an adiabatic passage, but in much shorter time than what is required for the adiabatic evolution; the so-called shortcuts to adiabaticity [20–22]. Here, as shown in Fig. 1(c), the detuning $\Delta \equiv (\omega_{R1} - \omega_{R2}) - (\omega_{HF} - \omega_X)$ and the amplitude Ω of Raman laser beams are swept by $\Delta(t) = \Delta_{ut}\cos(\pi t/T_{ut})$ and $\Omega(t) = \Omega_{ut}[\sin(\pi t/T) + i\beta]$, where the phase term $i\beta$ is the counter-diabatic term to suppress excitations during the fast evolution [20–22]. We evaluate the reliability of the uniform transfer by performing the Q-function measurements for the phonon number states $|n = 0, 1, 2\rangle$ as shown in Fig. 1(d). Here, we prepare the phonon number states $|n = 0, 1, 2\rangle$ and the displacing along one direction in phase space and we do not observe serious imperfection over our quantum projection noise.

The (anti)-JCM dynamics can be described by the time evolution $|\psi(t)\rangle = \exp\left(-itH_{(a)JC}/\hbar\right)|\beta\rangle$. We omit $\phi = 0$ in $H_{(a)JC}(\phi)$. Generally, two systems, a qubit and a

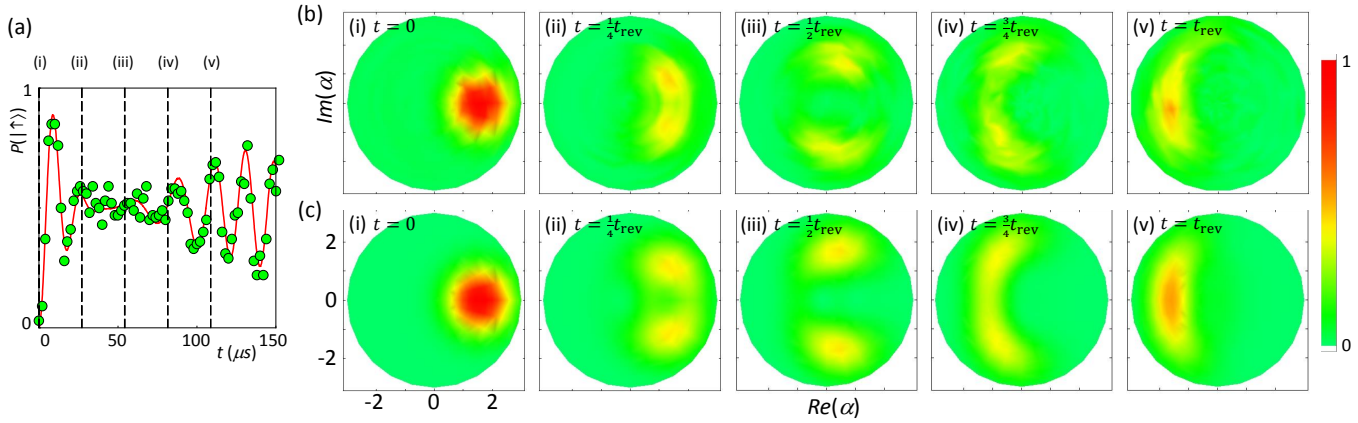

FIG. 2: **The time evolution of the Q-function for an initial coherent state under anti-JCM interaction.** (a) Collapse and revival of Rabi oscillation signal, (b) experimentally measured and (c) numerically calculated Q-functions of phonon field with the initial coherent state $|\beta = 1.62(0.05)\rangle$ depending on the duration of anti-JCM interaction (see Supplementary information section C). (a) $P(|\uparrow\rangle)$ is the probability of detecting the atom in $|\uparrow\rangle$. The points are experimental data after 100 repetitions. The solid line is from fitting the data with $\sum_{n=0} \frac{1}{2}\left[1 - \mathrm{e}^{-\gamma t}\cos\left(\sqrt{n+1}\eta\Omega t\right)\right]$, where γ is the empirical decay constant. At (b) and (c), the time for each snapshot of the Q-functions are labeled as (i)-(v) in the unit of the revival time t_{rev}, where $t_{\mathrm{rev}} = \frac{4\pi|\alpha|}{\eta\Omega} = 108.8\ \mu$s. In (b), each Q-function is obtained from 100 repetitions of the vacuum measurements after 384 different displacements, where the amplitude and the phase of displacement $|\alpha|\mathrm{e}^{i\varphi}$ are scanned from 0 to 3.0 with the step size of 0.2 and from 0 to 2π with the 24 steps, respectively.

phonon mode for our experiments, start interacting unless they are prepared in an eigenstate of the interaction Hamiltonian. It is natural to expect that they would be entangled by the interaction. It was, however, found that the atom and the field in the JCM or anti-JCM are nearly disentangled during the course of interaction if the atom is initially prepared in a superposition of $|\uparrow\rangle$ and $|\downarrow\rangle$ and the motion is initially in the coherent state $|\alpha\rangle$ of its amplitude α with $|\alpha| \gg 1$. Let us consider the initial state of the atom $|\Psi_A^{\pm}\rangle = \left(|\uparrow\rangle \mp i\,|\downarrow\rangle\right)/\sqrt{2}$. By the interaction (1), the atom-phonon state evolves to $|\Psi_{A-P}^{\pm}(t)\rangle = |\Psi_P^{\pm}(t)\rangle \otimes |\Psi_A^{\pm}(t)\rangle$ [23], where

$$|\Psi_A^{\pm}(t)\rangle = \left(\mathrm{e}^{\pm i\pi t/t_{\mathrm{rev}}}\,|\downarrow\rangle \mp i\,|\uparrow\rangle\right)/\sqrt{2} \qquad (2)$$

$$|\Psi_P^{\pm}(t)\rangle = \exp\left(\mp it\frac{\eta\Omega\sqrt{\hat{n}}}{2}\right)|\alpha\mathrm{e}^{\pm i\pi t/t_{\mathrm{rev}}}\rangle\,. \qquad (3)$$

From this, it is clear that if the atom is prepared in its ground state $|\downarrow\rangle$ $\left[= \left(|\Psi_A^-\rangle - |\Psi_A^+\rangle\right)/\sqrt{2}i\right]$, the atom-phonon state will be in the superposition of $|\Psi_{A-P}^{\pm}(t)\rangle$. The phonon state will rotate in phase space, where $t_{\mathrm{rev}} = \frac{4\pi|\alpha|}{\eta\Omega}$ is the corresponding revival time.

In the experiment, we prepare a coherent state of $|\beta\rangle = 1.62(0.05)$ with the internal state $|\downarrow\rangle$ by displacing the $|n=0\rangle$ state after the standard Raman-sideband ground-state cooling (see Supplementary information section A). Then we apply the Raman laser beams for the anti-JCM interaction and observe the dynamics of the atom and the field. For the internal state of atom, we measure the probability of being in the $|\uparrow\rangle$ state, $P\left(|\uparrow\rangle\right)$ by the standard fluorescence detection scheme. For the field, we choose five different interaction times $t = (0, \frac{1}{4}, \frac{1}{2}, \frac{3}{4}, 1)\ t_{\mathrm{rev}}$ in the anti-JCM. After the interaction time t, we displace the state by α and trace over the internal degree of freedom by the standard optical pumping sequence, which does not produce any noticeable change of the phonon distribution (see Supplementary information section B). Then we measure the vacuum component to reconstruct $Q(\alpha)$.

Figs. 2(b) and (c) show the experimental and theoretical time evolution of the initial coherent state under the anti-JCM interaction. The theoretical results are obtained by the numerical simulation of the master equation of anti-JCM Hamiltonian including experimental imperfections (see Supplementary information section C). At $t = 0$, $P(|\uparrow\rangle) = 0$ and $Q(\alpha)$ is Gaussian, which represents the coherent state. At time $t = t_{\mathrm{rev}}/4$, while Rabi oscillations begin to collapse, the Gaussian peak splits into two, which can be understood by the separation of two atom-phonon states $|\Psi_{A-P}^{\pm}\rangle$. The two components of the atom-phonon entangled state evolve in the opposite phases as shown in Eqs. (2) and (3). At the half revival time $t = t_{\mathrm{rev}}/2$, the two atomic states in Eq. (2) become identical except the global phase, which results in disentanglement of the atomic state from the phonon state (see Fig. 3 for an experimental evidence). In the Q-function, the phonon state shows two clearly separated peaks that are located at the opposite phases in phase space. This can be understood as the superposition of two coherent states [23]. The further evolution of the phonon state is shown in Fig. 2(iv) and (v). At the revival time $t = t_{\mathrm{rev}}$, the two phonon peaks merge at the opposite position

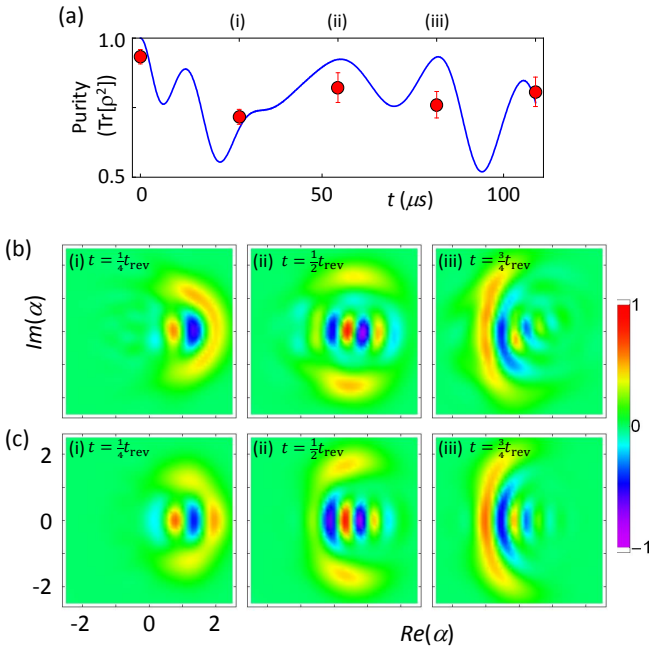

FIG. 3: **Purity and the Wigner function.** (a) The purities $\mathrm{Tr}\left(\rho^2\right)$ are measured from the reconstructed density matrix. The error bars are obtained by the Monte-Carlo simulation of reconstructing density matrix from the measured phonon distributions with experimental uncertainties. The solid line comes from the numerical calculation of the master equation of the anti-JCM Hamiltonian (see Supplementary information section C). At t=$t_{\mathrm{rev}}/2$, the purity is 0.82(0.05), which is expected to be higher when $\beta \gg 1$. This high purity shows that at t=$t_{\mathrm{rev}}/2$ the phonon state is nearly disentangled with the internal state and maintains its coherence. The experimental results (b) and theoretical predictions (c) of the Wigner function are plotted. The interaction times of the anti-JC coupling are shown on top of each panel as (i)-(iii). The experimental results are in good agreement with the theory. The negativity of the Wigner function indicates the emergence of nonclassical state during the dynamic evolution.

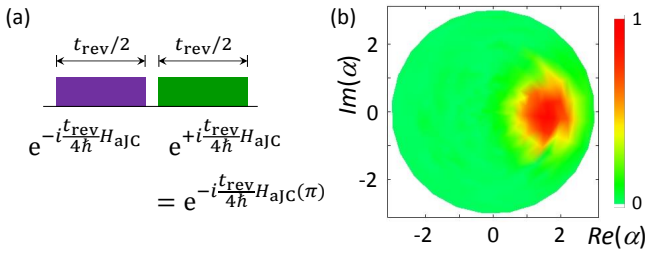

FIG. 4: (a) Generalized echo-sequence the time reversal of anti-JCM evolution for the interaction time $t = t_{\mathrm{rev}}/2$. The $\phi = \pi$ phase of the anti-JCM Hamiltonian produces the negative sign; $H_{\mathrm{aJC}}(\pi) = -H_{\mathrm{aJC}}(0)$, which performs the time reversal operation. (b) The measured Q-function of the phononic state after time reversal operation of (a). The total number of measurements for the Q-function reconstruction is same as that in Fig. 2.

of the initial coherent state, which causes the revival of Rabi oscillations. Due to the quadratic phase term in Eq. (2), the amplitude of the Rabi oscillations is reduced (see Supplementary information section D).

In order to further test that the two peaks in phase space at $t = t_{\mathrm{rev}}/2$ correspond to the two composite states in coherent superposition, we need to fully determine the state of the phonon field. In principle, this can be done from the measured Q-function. However, since the amplitude of the interference is extremely small and the values never become negative in the Q-function [8, 16, 24], it is difficult to observe quantum coherence of the coherent superposition. We thus reconstruct the density matrix and the Wigner function of the phononic state [22], by applying the iterative maximum-likelihood method [25] to avoid unphysical, non-positive density matrix. We displace the state to 8 different angles with the amplitude ≈ 0.8 and obtain the phonon number distributions by the fitting of Rabi-oscillations of anti-JCM [18, 26]. The density matrix is then used to reconstruct the Wigner function.

Fig. 3 shows the reconstructed Wigner functions at the interaction times $t = (\frac{1}{4}, \frac{1}{2}, \frac{3}{4})\ t_{\mathrm{rev}}$, which are compared with the numerically obtained ones from the master equation. Other than $t = 0$ and t_{rev}, the interference fringes with negative values are clearly observed, which strongly indicates that the phonon packets are non-classical quantum states in coherent superposition. We also measure the purities of the states from the density matrix as shown in Fig. 3(a). The purity goes up at $t = t_{rev}/2$ but not near to unity, due to the fact that the initial amplitude of the coherent state is small.

We perform the time reversal operations, which force the evolved phonon state evolved under the anti-JCM interaction to retrace its past trajectory in the opposite direction by the generalized echo scheme [27]. For the echo method [10], we introduce a π phase shift in the second half of the anti-JCM interaction, *i.e.*, $\mathrm{e}^{-i\frac{t}{2\hbar}H_{\mathrm{aJC}}(\pi)} = \mathrm{e}^{+i\frac{t}{2\hbar}H_{\mathrm{aJC}}}$. We apply the reverse process at the half revival time $t = t_{\mathrm{rev}}/2$ and confirm the process by measuring the Q-function of the final phonon state. Keeping the coherence of the interaction is at the heart of the time reversal we show in Fig. 4. We note that there is other way of reversing the anti-JCM by applying the JCM, which is discussed in the supplementary information [28].

We have shown a highly efficient scheme to detect the vacuum which is used to reconstruct the dynamics of the JCM field for the first time. In our experimental demonstration, the size of the initial coherent state $|\beta\rangle$ could be increased by improving our ion trap system in which way the approximated analytical theory can be better compared with experimental data. The main current limitation comes from the unreliable displacement operation for a large scale above $\alpha \approx 4.8$, which is caused by the

heating of the phonon mode. The reduction of an order of magnitude in the heating rate would allow us to reach an order of magnitude large phonon number state. Our developed technique of Q-function measurement can be performed in a single detection and used to probe many other dynamics of the phonon field. Our approach is generic and would also be applied to other physical platforms including opto-mechanics and circuit-QED system.

Acknowledgement

This work was supported by the National Basic Research Program of China under Grants No. 2011CBA00300 (No. 2011CBA00301), the National Natural Science Foundation of China 61073174, 61033001, 61061130540, and 11374178. K. Kim acknowledges the first recruitment program of global youth experts of China. M.S. Kim was supported by the UK EPSRC and Royal Society.

*m.kim@imperial.ac.uk
†kimkihwan@gmail.com

[1] E. T. Jaynes and F. W. Cummings, Proceedings of the IEEE **51**, 89 (1963).
[2] J.H. Eberly, N.B. Narozhny, and J.J. Sanchez-Mondragon, Phys. Rev. Lett. **44**, 1323 (1980).
[3] S. P. D. Phoenix and P. L. Knight, Annals of Physics **186**, 381 (1988).
[4] J. Gea-Banacloche, Phys. Rev. Lett. **65**, 3385 (1990).
[5] J. Gea-Banacloche, Phys. Rev. A **44**, 5913 (1991).
[6] J. Eiselt and H. Risken, Optics communications **72**, 351 (1989).
[7] J. Eiselt and H. Risken, Phys. Rev. A **43**, 346 (1991).
[8] J.-M. Raimond and S. Haroche, *Exploring the quantum* (Oxford University Press, 2006).
[9] A. Auffeves, P. Maioli, T. Meunier, S. Gleyzes, G. Nogues, M. Brune, J.-M. Raimond, and S. Haroche, Phys. Rev. Lett. **91**, 230405 (2003).
[10] J.-M. Raimond, T. Meunier, P. Bertet, S. Gleyzes, P. Maioli, A. Auffeves, G. Nogues, M. Brune, and S. Haroche, J. Phys. B: At. Mol. Opt. Phys. **38**, S535 (2005).
[11] K. E. Cahill and R. J. Glauber, Phys. Rev. Lett. **177**, 1882 (1969).
[12] C. Monroe, D. Meekhof, B. King, and D. Wineland, Science **272**, 1131 (1996).
[13] M. Brune, E. Hagley, J. Dreyer, X. Maitre, A. Maali, C. Wunderlich, J.-M. Raimond, and S. Haroche, Phys. Rev. Lett. **77**, 4887 (1996).
[14] S. Deleglise, I. Dotsenko, C. Sayrin, J. Bernu, M. Brune, J.-M. Raimond, and S. Haroche, Nature **455**, 510 (2008).
[15] M. Hofheinz, H. Wang, M. Ansmann, R. C. Bialczak, E. Lucero, M. Neeley, A. D. O'Connell, D. Sank, J. Wenner, J. M. Martinis, et al., Nature **459**, 545 (2009).
[16] G. Kirchmair, B. Vlastakis, Z. Leghtas, S. E. Nigg, H. Paik, E. Ginossar, M. Mirrahimi, L. Frunzio, S. M. Girvin, and R. J. Schoelkopf, Nature **495**, 205 (2013).
[17] B. Vlastakis, G. Kirchmair, Z. Leghtas, S. E. Nigg, L. Frunzio, S. M. Girvin, M. Mirrahimi, M. H. Devoret, and R. J. Schoelkopf, Science **342**, 607 (2013).
[18] D. Leibfried, D. M. Meekhof, B. E. King, C. Monroe, W. M. Itano, and D. J. Wineland, Phys. Rev. Lett. **77**, 4281 (1996).
[19] S. Barnett and P. M. Radmore, *Methods in theoretical quantum optics* (Oxford University Press, 1997).
[20] M. Berry, Journal of Physics A: Mathematical and Theoretical **42**, 365303 (2009).
[21] J. Zhang, J. Zhang, X. Zhang, and K. Kim, Phys. Rev. A **89**, 013608 (2014).
[22] M. Um, J. Zhang, D. Lv, Y. Lu, S. An, J.-N. Zhang, H. Nha, M. S. Kim, and K. Kim, arXiv:1506.07268 (2015).
[23] V. Bužek, H. Moya-Cessa, P. L. Knight, and S. J. D. Phoenix, Phys. Rev. A **45**, 8190 (1992).
[24] M. S. Kim and V. Bužek, Phys. Rev. A **46**, 4239 (1992).
[25] J. Řeháček, Z. Hradil, and M. Ježek, Phys. Rev. A **63**, 040303 (2001).
[26] D. M. Meekhof, C. Monroe, B. E. King, W. M. Itano, and D. J. Wineland, Phys. Rev. Lett. **76**, 1796 (1996).
[27] M. H. Levitt, *Spin dynamics: basics of nuclear magnetic resonance* (John Wiley & Sons, 2001).
[28] B.M. Rodriguez-Lara, H. Moya-Cessa, and A.B. Klimov, Phys. Rev. A **71**, 023811 (2005).